Sensitivity of the frozen-melted basal boundary to perturbations of basal traction and geothermal heat flux: Isunnguata Sermia, western Greenland

Douglas J. BRINKERHOFF,[1] Toby W. MEIERBACHTOL[2], Jesse V. JOHNSON,[1] Joel T. HARPER,[2]

[1]*Department of Computer Science, University of Montana, 32 Campus Avenue, Missoula, MT 59812, USA*

E-mail: douglas.brinkerhoff@umconnect.umt.edu

[2]*Department of Geosciences, University of Montana, 32 Campus Avenue, Missoula, MT 59812, USA*

ABSTRACT. A full-Stokes, thermo-mechanically coupled, numerical model is used to explore the interaction between basal thermal conditions and motion of a terrestrially terminating section of the west Greenland ice sheet. The model domain is a two-dimensional flow-line profile extending from the ice divide to the margin. We use data assimilation techniques based on the adjoint model in order to optimize the basal traction field, minimizing the difference between modelled and observed surface velocities. We monitor the sensitivity of the frozen-melted boundary (FMB) to changes in prescribed geothermal heat flux and sliding speed by applying perturbations to each of these parameters. The FMB shows sensitivity to the prescribed geothermal heat flux below an upper threshold where a maximum portion of the bed is already melted. The position of the FMB is insensitive to perturbations applied to the basal traction field. This insensitivity is due to the short distances over which longitudinal stresses act in an ice sheet.

INTRODUCTION

At geologic time scales, high latitude countries in the Northern Hemisphere will likely experience future glaciations. The long term storage of nuclear waste in deep geologic repositories can potentially be impacted by a glaciation via the ice sheet's

influence on the subglacial and proglacial groundwater system. It is therefore important to consider subglacial hydrological processes and the role ice sheets play in driving groundwater systems when designing safe storage systems in northern locations. Subglacial hydrological processes become active and recharge the groundwater system only where the bed of an ice sheet is melted. Understanding the spatial pattern of thermal conditions of an ice sheet's bed is therefore an important design criteria for responsible nuclear waste disposal in countries like Sweden, Finland and Canada.

The Greenland Ice Sheet (GrIS) is a present day analog to future ice sheets in Scandinavia and Canada. The thermal state of the bed of GrIS and the accumulation of subglacial water has been investigated by a variety of methods, but remains poorly constrained. Direct observations via drilling show that melted conditions exist near the western margin (Luthi et al., 2002), as well as at a north-central location near the ice sheet divide. Conversely, frozen conditions have been noted at point locations spanning the ice sheet from Camp Century near the northwest margin (Weertman, 1968), to the centrally located GRIP core, and the southeast Dye 3 core (Dahl-Jensen et al., 1998). The spatial extent of melted bed conditions as determined by the few point observations has been extended via interpretation of ice penetrating radar. Fahnestock et al. (2001) derived spatially variable basal melt rates exceeding 0.15 ma^{-1} in central GrIS through interpretation of internal radar layering. Using bed reflectivity power as a proxy for basal water content, Oswald and Gogineni (2008) suggested a spatially heterogenous basal water distribution along radar transects of the GrIS.

Spatially comprehensive estimates of basal conditions are offered by ice sheet model output. Greve (1997) investigated the sensitivity of the basal temperature field on the Greenland ice sheet to variations in a uniform geothermal heat flux. His results suggested that, while increasing heat flux caused an inland migration of temperate basal conditions, the interior remained frozen, even under the highest heat flux scenario (54.6 mWm^{-2}). This was complemented by a follow-up investigation of the basal temperature field by matching geothermal heat flux to point observations, which implied that the majority of the ice sheet bed was at the pressure melting point (Greve, 2005). In addition to geothermal heat flux, the sensitivity of GrIS basal conditions to changes in surface temperatures and mass balance was investigated by Huybrechts et al. (1996), who found that basal conditions show a pronounced sensitivity to steady state changes to temperature and mass balance; *e.g.* a 10°C drop in surface temperature resulted in a freezing of the majority of the ice sheet bed, however, the drop in surface mass balance associated with a 10°C lowering of surface temperature resulted in temperate conditions over nearly 60 percent of the bed. Transient simulations over the last two glacial cycles showed most of GrIS exhibits frozen conditions at the bed at some point in time. While the models employed by both Greve and Huybrechts were three-dimensional, both were mechanically limited to the shallow ice approximation.

In summary, previous studies suggest a spatially distinct frozen-melted boundary (FMB). The location of the FMB at the bed is the result of a balance between heat sources concentrated near the bed (frictional heat from sliding, geothermal

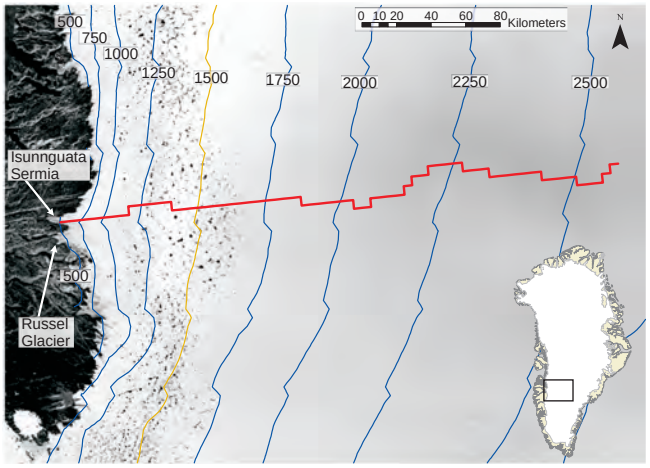

Fig. 1. Study site displaying model profile (red line) from the ice sheet divide through Isunnguata Sermia to the western margin. Surface elevation contours (blue lines) are given in meters above sea level, and interpolated from Bamber et al(2001). Yellow contour at 1500 m a.s.l. represents the approximate equilibrium line altitude (ELA) according to van de Wal et al. (2008).

heat flux, and strain heating), and the introduction of colder ice through diffusive and advective processes. In the present study, we investigate the sensitivity of the FMB not only to geothermal heat flux, but also to changes in cold ice advection resulting from ice motion, including basal sliding. Sensitivity is investigated with a steady-state, thermomechanically coupled, two-dimensional flow line model which solves the Stokes equations. We apply this model to a profile of Issunnguata Sermia, a terrestrially terminating glacier in western GrIS. The model is brought into agreement with observation by using adjoint methods for evaluating gradients of an objective function. Motivation for selecting a terrestrially terminating glacier stems from the fact that the majority of the GrIS is land terminating, and such a profile removes additional physical complexities relating to marine-terminating ice. Using the steady state glacier geometry and surface velocity field, we examine the interactions of heat sources that dictate the stability of the FMB under different assumptions about geothermal heat flux and the basal traction fields.

METHODS

Field equations

Our model is built upon the continuum mechanical formulation of the laws of conservation of mass, momentum, and energy for an incompressible fluid. These are, respectively;

$$\nabla \cdot \mathbf{u} = 0, \tag{1}$$

$$\frac{d\mathbf{u}}{dt} = \nabla \cdot \sigma + \rho \mathbf{g}, \tag{2}$$

Parameter	**Symbol**	**Value**
Gravitational acceleration	$\mathbf{g}$	9.81 m/s^2
Thermal conductivity of ice	k_i	2.1 W/m K
Density of ice	ρ	911 kg/m^3
Heat capacity of ice	c_p	2093 J kg^{-1}K^{-1}
Latent heat of fusion of ice	L	3.35×10^5 J kg^{-1}
Triple point of water	T_0	273.15 K
Pressure dependence of melting	β	-9.8×10^{-8} K/Pa
Universal gas constant	R	8.314 J/mol K
Seconds per year	-	31556926 s a^{-1}
Glen's flow law exponent	n	3
Viscosity regularization	$\dot{\epsilon}$	10^{-30} Pa s

Table 1. Parameters and physical constants used in the model.

$$\frac{d\theta}{dt} = \frac{1}{\rho c_p}\nabla \cdot k_i \nabla\theta - \mathbf{u}\cdot\nabla\theta + \Phi. \tag{3}$$

$\mathbf{u}$ represents the velocity vector, σ the stress tensor, θ the temperature, and Φ sources of heat generation in the ice. Physical constants c_p, k_i, ρ, and $\mathbf{g}$ are defined in Table 1. Analysis is restricted to the xz plane, or the vertical profile, making $\nabla = \frac{\partial}{\partial x}\hat{\imath} + \frac{\partial}{\partial z}\hat{k}$. $\hat{\imath}$ and $\hat{k}$ are unit vectors in the x and z directions, respectively.

Conservation of momentum

The constitutive relation for ice takes the form

$$\tau_{ij} = 2\eta\dot{\epsilon}_{ij}, \tag{4}$$

τ_{ij} is the ij element of the deviatoric stress tensor, which is defined by $\tau_{ij} = \sigma_{ij} - p\delta_{ij}$, and δ_{ij} is the Kronecker delta function. $\dot{\epsilon}_{ij}$ represents the corresponding element of the strain rate tensor, p the pressure, and η the viscosity. The strain rate tensor is given by, and related to velocity gradients as follows

$$\dot{\epsilon}_{ij} = \frac{1}{2}\left(\frac{\partial u_i}{\partial x_j} + \frac{\partial u_j}{\partial x_i}\right). \tag{5}$$

A non-Newtonian rheology is used for ice

$$\eta = \frac{1}{2}A(\theta^*)^{-1/n}(\dot{\epsilon}_{\mathrm{II}} + \dot{\epsilon}_0)^{(1-n)/n}, \tag{6}$$

with $\dot{\epsilon}_{\Pi}^2 = \frac{1}{2}\Sigma_{ij}\dot{\epsilon}_{ij}\dot{\epsilon}_{ij}$, or the second invariant of the strain rate tensor, and $\dot{\epsilon}_0$ is a regularization parameter introduced to avoid a singularity at zero strain rate. Glen's flow law (Paterson, 1994) gives n =3. $A(\theta^*)$ is the flow law rate factor, given by Paterson and Budd (1982).

$$A(\theta^*) = \begin{cases} 3.61 \times 10^{-13} \quad \mathrm{e}^{-6.0\times10^4/R\theta^*}, & \theta^* \leq 263.15\mathrm{K}, \\ 1.73 \times 10^{3} \quad \mathrm{e}^{-13.9\times10^4/R\theta^*}, & \theta^* > 263.15\mathrm{K}, \end{cases} \tag{7}$$

where θ^* is the homologous temperature, defined by $\theta^* = \theta + \beta p$, and R the universal gas constant.

Under the assumption of steady state, the velocity of the ice is then given by the following equation:

$$-\nabla \cdot [\tau - p\mathbf{I}] = \rho\mathbf{g} \tag{8}$$

Conservation of energy

Φ, the term in Equation 3 which represents internal heat generation, is computed as

$$\Phi = 2\eta\dot{\epsilon}_{\Pi}^2. \tag{9}$$

Under the assumption of steady state, and uniform thermal conductivity, the temperature of the ice is given by the following equation:

$$0 = \frac{k_i}{\rho c_p}\nabla^2\theta - \mathbf{u}\cdot\nabla\theta + 2\eta\dot{\epsilon}_{\Pi}^2. \tag{10}$$

Boundary Conditions

Boundary conditions are applied to three distinct regions on the boundary of Isunnguata Sermia; (1) the surface, (2) the bed, and (3) a vertical boundary at the ice divide.

Conservation of Momentum and Mass Boundary Conditions

The surface of the glacier upholds the neutral or stress free boundary condition

$$[\tau - p\mathbf{I}]\hat{\mathbf{n}} = 0, \tag{11}$$

where $\hat{\mathbf{n}}$ is the outward normal unit vector.

The bed of the glacier is subjected to a Weertman style sliding law, where basal velocity and shear stress are related as

$$\tau_b = \beta^2\mathbf{u} \tag{12}$$

where β^2 is a scalar, spatially variable parameter representing the magnitude of frictional forces at the bed, and τ_b is given by

$$\tau_b = \sigma \hat{\mathbf{n}} \tag{13}$$

evaluated at the base of the glacier,

The vertical boundary at the divide, is subject to a symmetry boundary condition,

$$\hat{\mathbf{n}} \cdot \mathbf{u} = 0 \tag{14}$$

$$[\tau - p\mathbf{I}] \cdot \hat{\mathbf{t}} = 0. \tag{15}$$

Where $\hat{\mathbf{t}}$ is the unit vector tangent to the boundary.

Conservation of Energy Boundary Conditions

The bed of the glacier is subject to an inward heat flux given by

$$Q = q_g + q_f - q_l \tag{16}$$

where q_g is the geothermal heat flux, q_f is heating due to sliding friction, and q_l is latent heat associated with the melting of ice. q_g is a prescribed value of 42mW/m^2, unless otherwise stated. Frictional heat is calculated as

$$q_f = \mathbf{u} \cdot \tau_\mathbf{b}. \tag{17}$$

Latent heat is given by

$$q_l = \begin{cases} q_f + q_g + k_i \frac{\partial \theta}{\partial z}, & \theta^* \geq 273.15 \\ 0, & \theta^* < 273.15 \end{cases} \tag{18}$$

This heat interacts with the ice via the Neumann boundary condition

$$-\hat{\mathbf{n}} k_i \nabla \theta = Q. \tag{19}$$

Note that the inclusion of the latent heat term serves as a temperature constraint on the ice by counteracting the inward flux from geothermal heat and frictional heat when the basal ice is at the pressure melting point.

The surface temperature of the glacier is inferred from the dataset of Ettema et al. (2009), and is imposed as a Dirichlet boundary condition. The vertical boundary at the divide is thermally insulated such that $\hat{\mathbf{n}} \cdot [-k_i \nabla \theta] = 0$.

Quantity	**Value**
Mesh Elements	632
Degrees of Freedom	4686
Element Type	Lagrange Quadratic
Initial Damping Factor	1×10^{-4}
Minimum Damping Factor	1×10^{-8}
Criterion for Convergence	$<1\times10^{-6}$

Table 2. Quantities of importance for model numerics.

Model Domain

The geometry for the model domain was derived from surface elevation and thickness data of Bamber et al. (2001). Since the model used here considers only a vertical profile, we selected a streamline from the surface velocity data presented in Joughin et al. (*In press*). We employed cubic splines to interpolate the glacier geometry between data points, which were spaced at 5 kilometers.

Due to the discrete nature of the original dataset, the profile surface contained numerous artifacts, manifested as irregularities in slope. In order to produce a more reasonable surface, we implemented a free-surface evolution scheme, and allowed the model geometry to relax for 50 years. The high driving stresses associated with the slope irregularities quickly diffused, yielding a surface free from the original artifacts, and still consistent with the data and model physics.

Numerical Considerations

The model uses the finite element method to solve the field equations subject to the boundary conditions. Lagrange quadratic elements are used (Hughes, 2000), allowing second derivatives of the velocity to be computed accurately. The non-linearity resulting from the viscosity (Equation 6) is resolved by using the modified Newton's method iterative solver (Deuflhard, 1974). The resulting linear systems were solved with UMFPACK (Davis, 2004). Model specific parameters are summarized in Table 2. All numerical work was carried out in the *Comsol Multiphysics* modeling environment, a commercial package for finite element analysis of general partial differential equations.

Modeling assumptions

Several assumptions were made in the development of this model, and results must be understood with these in mind. These assumptions are as follows:

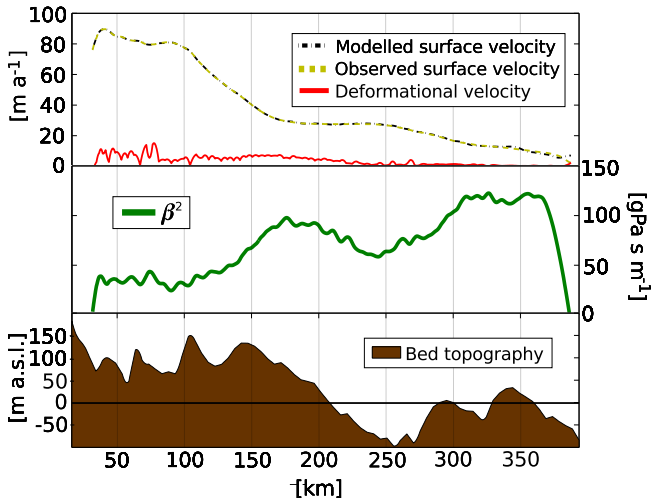

Fig. 2. Top panel shows the modelled and observed velocity, as well as the portion of the modelled velocity accounted for by internal deformation. The middle panel shows the β^2 field derived from the data assimilation procedure. The lowest panel shows the topography underlying the modelled ice profile.

1. The data sets used in the generation of the model domain geometry are sufficiently accurate, and the surface smoothing used to reduce artifacts does not introduce additional errors larger than those resulting from artefacts in surface geometry.

2. Stresses acting transverse to the dominant flow direction are small. This is necessary due to the effect that these stresses, and associated strains, have on the rheologic properties of the ice. Given the profile's location at the center of the ice catchment, and the uniform width of the streaming feature, this assumption is likely valid.

3. The steady steady state solution generated by the data assimilation process is a reasonable representation of a long term configuration for the model domain. This assumes that the modeled region of the GrIS was not in a transient state at the time that data was collected.

4. A constant geothermal heat flux is an appropriate parameterization of the real phenomenon across the modelled domain. This is to say that given the spatial scale under consideration, variability in geothermal heat flux is either of a sufficiently low resolution to be considered in an average sense, or of a sufficiently large scale that it is essentially constant.

5. Steady state solutions which include the data assimilation process are sufficient for probing the sensitivities of the system with respect to changes in the basal boundary. A more complete treatment would entail the evolution of the free surface to determine the ultimate outcome of the perturbation, but that is beyond the scope of this work.

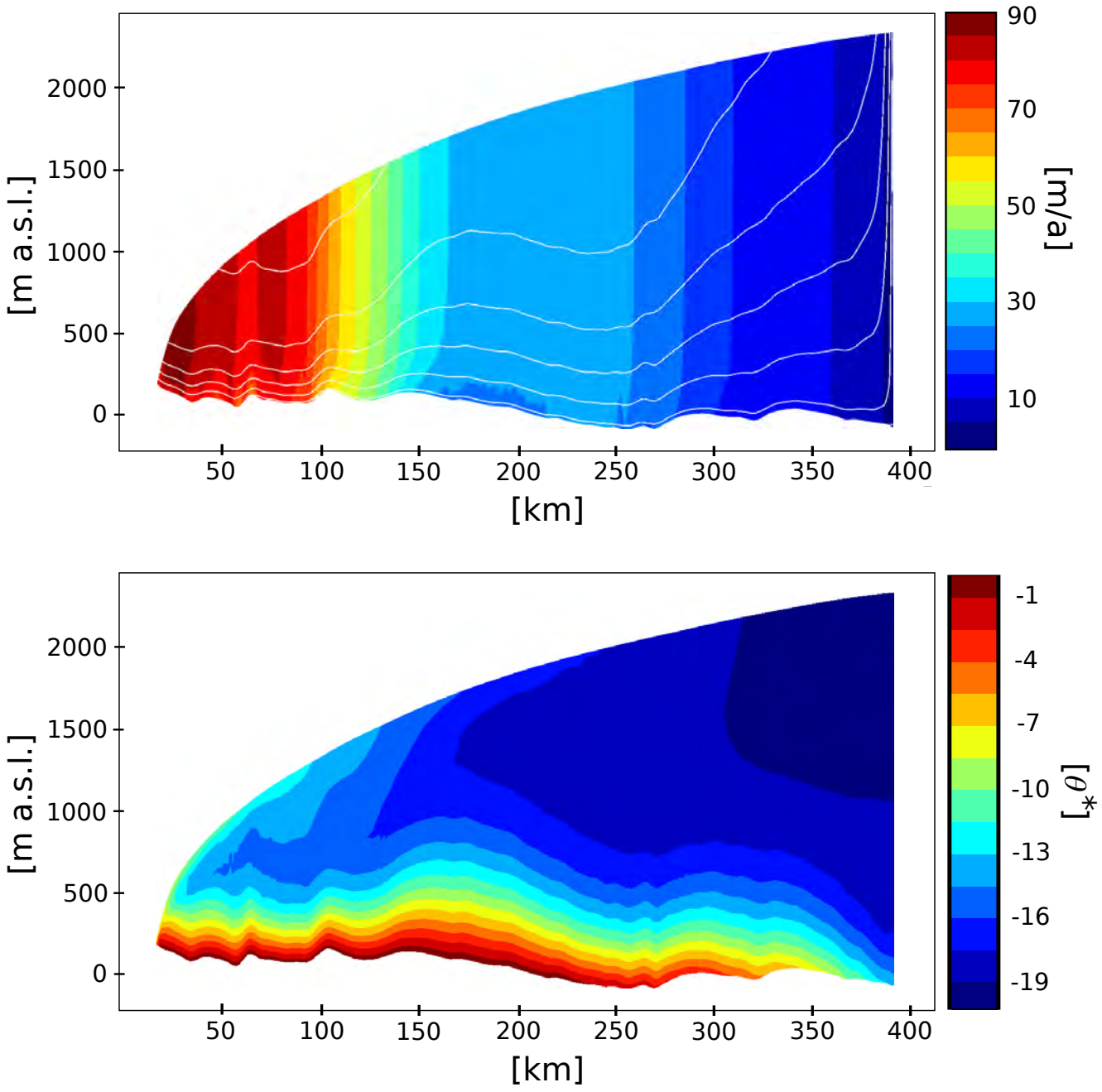

Fig. 3. The velocity (top) and temperature (bottom) fields produced by the data assimilation process. White lines on the velocity figure indicate flowlines within the velocity field

Data assimilation and model initialization

When modeling ice dynamics, there are two issues that must be addressed before numerical experiments can be conducted. First, fields which have not been directly measured but are significant in computing flow must be estimated. For instance, the internal distribution of temperatures are critical to ice dynamics, but are at best known at a few boreholes. We will refer

to this process as model initialization. Secondly, the initialized model should be in agreement with measurements that are available. We refer to this as data assimilation.

Our strategy in this paper will be to use steady state solutions to conservation equations to initialize the model subject to the constrains introduced by the data assimilation process. This is not a new idea, MacAyeal (1993) introduced control methods in the context of ice sheet modeling. Here, we extend the concepts to full Stokes solutions.

For data assimilation, we use the adjoint of the linear operator to compute derivatives of an objective function, and use those slopes to minimize the function. We have defined an objective function in terms of difference between the observed, $u^{\text{obs}}(\mathbf{x})$, and modeled, $u^{\text{mod}}(\mathbf{x})$ surface velocities,

$$g(u,p) = \sum_{i=1}^{N} (u^{\text{obs}}(\mathbf{x_i}) - u^{\text{mod}}(\mathbf{x_i}))^2 \tag{20}$$

which will be differentiated with respect to a parameter p that we vary in order to minimize the objective function. In this case the parameter will be $p = \beta(x)^2$ or the basal traction. Our discussion follows that of Strang (2007, pages 678-684).

'Chain rule' differentiation yields

$$\frac{dg}{dp} = \frac{\partial g}{\partial u}\frac{\partial u}{\partial p} + \frac{\partial g}{\partial p}, \tag{21}$$

where u is a solution vector containing both velocities and temperatures. The key to efficient calculation of the derivatives of the objective function is writing

$$\frac{\partial g}{\partial u} = c^T \tag{22}$$

or, recognizing that the objective function is linear in u. It is now possible to write the gradient as

$$\frac{dg}{dp} = c^T \frac{\partial u}{\partial p} + \frac{\partial g}{\partial p} = c^T A^{-1} \frac{\partial b}{\partial p} + \frac{\partial g}{\partial p}, \tag{23}$$

where that $c^T A^{-1}$ is the result of solving the "adjoint" linear system $A^T \lambda = c$ for $\lambda^T = c^T A^{-1}$. Note that the original problem is assumed to represented by the system of linear equations $Au = b$. Hence, the gradient for each step of an optimization algorithm (we use quasi-Newton) requires a single extra linear solve, rather than a linear solve for each of the many parameters, p. This savings makes it possible to do large inverse problems, such as computing a basal traction for each point in the model domain (see Fig. 2). Figure 3 then corresponds to the initialized velocity and temperature field, or the steady state solutions to the field equations that assimilate the data. This will provide the starting point for all numerical experiments. In some cases, such as determination of the sensitivity to q_g, the entire assimilation/initialization process is repeated with different values.

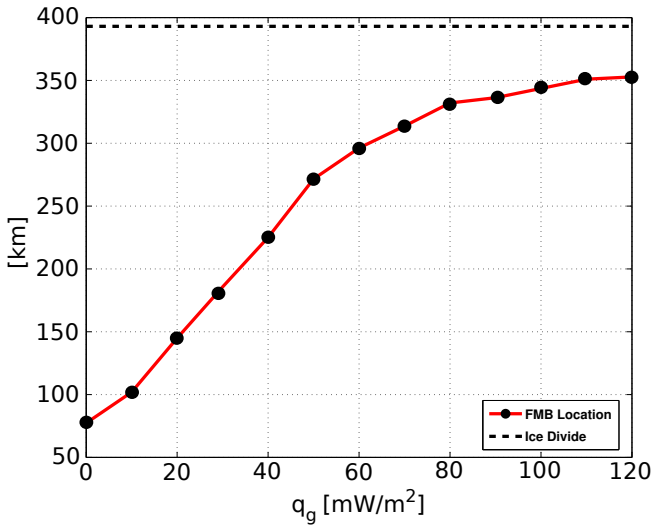

Fig. 4. Sensitivity of FMB location to variations in the geothermal heat flux.

NUMERICAL EXPERIMENTS

Sensitivity of the FMB to basal heat flow

In order to determine the sensitivity of the location of the FMB to different values of geothermal heat flux, we performed the data assimilation procedure over a range of possible values. This experiment is motivated by the observation that basal sliding represents a significant portion of the total modelled surface velocity, and we wished to determine the geothermal heat flux required to produce a completely melted bed, in line with the assumption that the bed must be at the melting point for sliding to occur. We conducted model runs at every 5mW/m^{2}within the range 0-120mW/m^2. Figure 4 shows the location of the FMB as a function of the prescribed geothermal heat flux. The FMB asymptotically approaches the divide as geothermal heat flux is increased, although the entire bed is not at the melting point under any of the parameter values considered, even for fluxes which seem unreasonably high. For comparison, previous authors have used a value of 42mW/m^2(Pattyn, 2003), and a structural similarity model by Shapiro and Ritzwoller (2004) indicates a mean geothermal heat flux of around 58mW/m^{2}along our flowline.

Sensitivity of the FMB to sliding

Previous work suggests that seasonal changes in the glacial drainage system below the ELA can contribute to changes in basal traction, leading to changes in surface velocity (van de Wal et al., 2008; Bartholomew et al., 2010; Joughin et al., 2008; Zwally et al., 2002). There is little agreement between these papers regarding the magnitude of proposed changes in surface velocity. Joughin et al. (2008) suggests that terrestrially terminating glaciers in the region south of Jakobshavn Isbrae (of which Isunnguata Sermia is one) experience 25% increases in surface velocity as a result of surface melt water lubricating the bed. Bartholomew et al. (2010) suggest speed-ups as great as 200%, and that a warming climate and associated surface lowering will

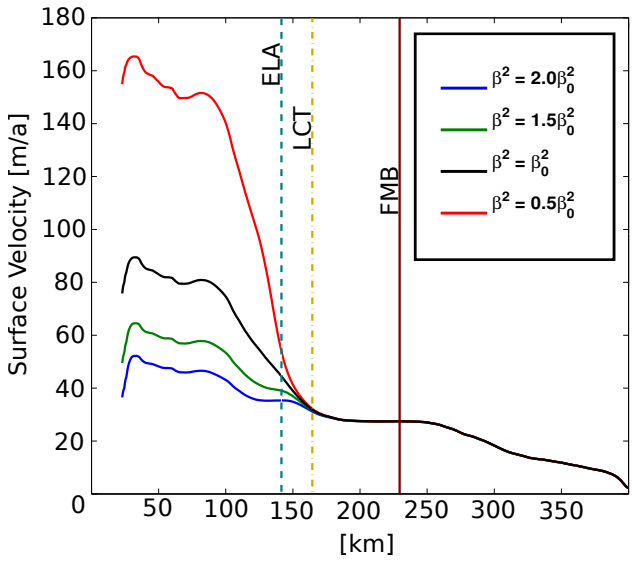

Fig. 5. Sensitivity of surface velocity to perturbations to the basal traction field, β^2. Equilibrium line altitude (ELA) is approximately 1500ma.s.l. We interpret the longitudinal coupling threshold (LCT) to be the location at which the difference between any two surface velocity profiles is $\leq$1 m/a.

expose greater portions of the bed to surface melt water, increasing the fraction of the ice sheet exposed to summer speed-ups. van de Wal et al. (2008) acknowledge these seasonal variations, but present data which show an overall 10% decrease in surface velocities between 1990 and 2007. They also note that surface ablation and velocity show no correlation.

Regardless of the magnitude and sign of such changes in surface velocity, we sought to determine whether perturbations to the basal traction field, β^2, downstream from the ELA, such as those which would be induced by increased surface meltwater production, would have an impact on the basal thermal regime, specifically the location of the frozen melted boundary. We tested this by inflicting constant multiplicative perturbations to β^2 downstream from the ELA, ranging between 50% and 200% of the value produced by the data assimilation process. The location of the FMB was insensitive to all of these perturbations. The reason for this is shown in Figure 5. Noteable changes in the surface velocity ($>1\text{ma}^{-1}$) field extend only 20km, or around 10 ice thickness, upstream from the extent of the perturbation. Thus, the advection of heat away from the bed, the dominant mechanism accounting for heat flux at the bed as shown in Figure 6, is unchanged 90km upstream, at the location of the FMB. This short coupling distance within the velocity field is corroborated by other studies (Bartholomew et al., 2010; Price et al., 2008).

Heat budget

In order to track the dominant factors which dictate the thermal regime at the bed, we calculated a heat budget of sources and sinks in terms of flux to the ice sheet base. We performed this calculation for a model scenario with optimized β^2 and a geothermal heat flux of 42mW/m^2; results are displayed in Figure 6. Upstream of the FMB, frozen conditions are controlled

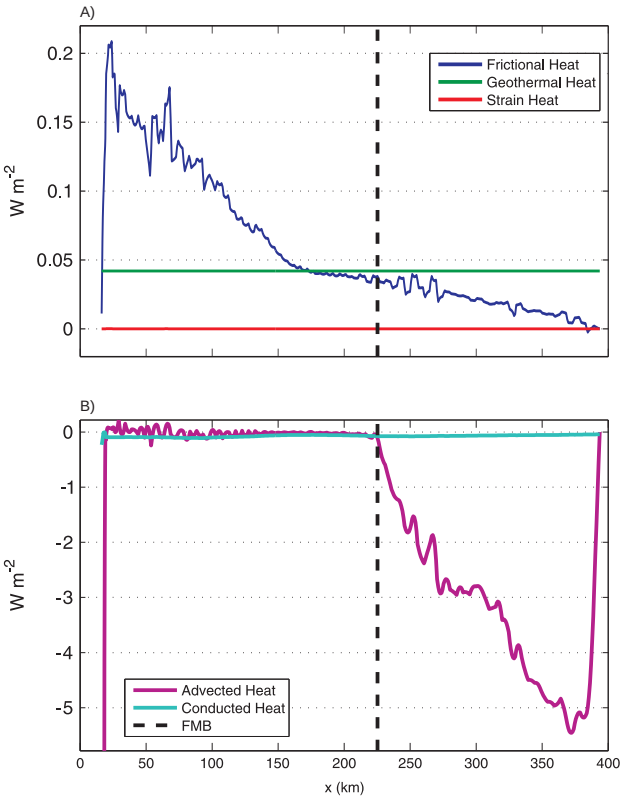

Fig. 6. Budget of heat sources (A) and sinks (B) along the profile basal boundary. Latent heat generation (not shown here), is a negative non-zero term below the FMB, and accommodates excess heat generated from (A). Strain heat is a positive non-zero term, but negligible compared to frictional and geothermal heat sources.

by the advection of cold ice. Near the divide, this advection is predominantly vertically directed from the surface. Moving downstream, advection becomes bed-parallel, so that advective flux decreases to zero at the FMB as heat sources raise the ice temperature as it flows along the bed. Throughout the frozen zone, and some kilometers beyond the FMB, the primary source of heat along the bed is geothermal heat flux. We find that heat generation due to straining at the bed is a positive contributor but negligible compared to geothermal and frictional sources. Downstream of the FMB, excess heat generation is accommodated by the consumption of latent heat associated with the phase transition from ice to water as basal melt occurs. Basal melting initiates at the FMB and steadily increases to a maximum of nearly 20 mm a^{-1} near the terminus.

DISCUSSION

The sensitivity experiments described above indicate strongly different responses by the FMB to perturbations in geothermal heat flux and basal sliding. The direct response of the basal thermal regime to changes in geothermal heat flux is an expected result. However the diminishing sensitivity of the FMB to increasingly higher heat fluxes is worth noting, and likely reflects the inability of the added heat to overcome cold advected from upstream.

In contrast, longitudinal coupling effects from sliding perturbations below the ELA do not propagate far enough up-glacier to influence the FMB. The location of the FMB is consequently insensitive to such perturbations. This interpretation hinges on the assumption that sliding perturbations apply only below the ELA which is reasonable considering that the effect of increased surface melt input to the basal hydrologic system is not likely to propagate a significant distance upstream along the bed. However, it is important to note that sliding in our model is not limited to below the ELA. In fact, our optimization scheme produces a β^2 field with sliding above the FMB to the ice divide, albeit the upstream sliding is small relative to that occurring near the margin. Migration of melted conditions to the divide does not occur under very high values of geothermal heat flux, thus the representation of sliding in our modeled frozen zone begs explanation.

If the bed is in fact frozen we see several potential explanations for our modeled sliding. First, sliding has been observed over a frozen bed consisting of a till layer (Engelhardt and Kamb, 1998), or hard bedrock (Echelmeyer and Wang, 1987; Cuffey et al., 1999). Additionally, substantial deformation has been observed within a frozen till layer, both within the body of the till itself, (Echelmeyer and Wang, 1987; Engelhardt and Kamb, 1998), as well as along discrete shear planes (Echelmeyer and Wang, 1987). This mechanism may be taking place if such a layer exists beneath GrIS. Second, and perhaps more likely, our model could under-represent velocity from ice deformation, requiring our optimization scheme to over-represent sliding to maintain the observed surface velocity. Changes in flow due to variable impurity and water content and grain size of ice is not accounted for in our model, however elsewhere in Greenland a layer of soft pre-Holocene ice has been observed to enhance flows by 1.7-3.5 fold (Paterson, 1994; Luthi et al., 2002). Alternatively, but in the same vein, the standard constitutive law we use could under-represent grain-scale ice deformation processes (Goldsby and Kohlstedt, 2001). Finally, the velocity field itself could potentially depict a velocity field out-of-balance with the current ice sheet geometry. We have no basis to eliminate any of these possibilities. However, if the magnitude of sliding over frozen bed computed here is not real, it is likely to be principally accounted for by spatial changes in geothermal heat flux, anisotropies within the ice, or a combination of the two.

An alternative scenario is therefore a partitioning of the observed surface velocity with enhanced ice deformation and reduced sliding velocity. Our heat budget along the basal boundary suggests the implementation of sliding has a significant influence on the location of the FMB by increasing the advection of cold ice along the bed. Under this alternative scenario, the associated drop in sliding velocity combined with additional interior heat generation from enhanced straining may modulate the cold contribution from advection, pushing the FMB further upstream. These processes would likely be countered by a decrease in frictional heating, which would force the FMB towards the margin. A model exploration of FMB migration from this interaction of heat sources is beyond the scope of this manuscript, and will be the focus of future work.

CONCLUSION

We developed a thermomechanically coupled, full-Stokes, 2-dimensional flowline model, which was applied to a terrestrially terminating glacier profile located in western Greenland. We extracted geometric information for the model domain from a dataset presented in Bamber et al. (2001), which we believe to be the best data available at present for the Greenland Ice Sheet. We used adjoint methods to optimize the basal traction field, such that modelled surface velocities matched observed values (Joughin et al., ress) to within 1ma^{-1}.

With an optimized model in hand, we conducted experiments in order to determine the sensitivity of the frozen-melted boundary (FMB) to perturbations in the basal heat flux and basal traction downstream the ELA. We found that the FMB migrates easily under different assumptions about geothermal heat flux. At values close to 0mW/m^2, the FMB moves very close to the terminus, but part of the bed remains unfrozen due to frictional heating from sliding. At high values, the FMB asymptotically approaches the ice divide. We found that for reasonable perturbations to basal traction downstream from the ELA, such as what might be expected from an increase in surface meltwater production and associated bed lubrication, the FMB was insensitive. This is a result of the short length scale over which longitudinal stress coupling in the ice operates ($\sim$10 ice thicknesses). The FMB is significantly further upstream from the ELA than the perturbations to the velocity field extend, thus advective heat fluxes are unchanged. Our model predicts that under most assumptions about geothermal heat flux, sliding occurs over a frozen bed. We see two possible explanations for this: 1) That this sliding is real, and follows one of the mechanisms proposed by Echelmeyer and Wang (1987), Engelhardt and Kamb (1998), or Cuffey et al. (1999), 2) Anisotropies within the ice resulting in a preferential flow direction and increased deformation. Additional work is needed to quantify the sensitivity of the basal thermal regime to the second of these factors.

ACKNOWLEDGEMENTS

Funding for this work was provided by the Greenland Analogue Project (GAP), a collaborative project funded by the nuclear waste management organizations in Sweden (Svensk Krnbrnslehantering AB), Finland (Posiva Oy) and Canada (NWMO). Partial funding for Johnson was also provided by NSF-CMG award 0934404.

REFERENCES

Bamber, J. L., Layberry, R. L., and Gogineni, S. P. (2001). A new ice thickness and bed data set for the greenland ice sheet 1. measurement, data reduction, and errors. *J. Geophys. Res.*, 106(D24):33773–33780.

Bartholomew, I., Nienow, P., Mair, D., Hubbard, A., King, M. A., and Sole, A. (2010). Seasonal evolution of subglacial drainage and acceleration in a greenland outlet glacier. *Nature Geosci*, advance online publication.

Cuffey, K. M., Conway, H., Hallet, B., Gades, A. M., and Raymond, C. F. (1999). Interfacial water in polar glaciers and glacier sliding at 17°C. *Geophys. Res. Lett.*, 26(6):751–754.

Dahl-Jensen, D., Mosegaard, K., Gundestrup, N., Clow, G. D., Johnsen, S. J., Hansen, A. W., and Balling, N. (1998). Past temperatures directly from the greenland ice sheet. *Science*, 282(5387):268–271.

Davis, T. (2004). A column pre-ordering strategy for the unsymmetric-pattern multifrontal method. *AMS Trans. Math. Software*, 30:165–195.

Deuflhard, P. (1974). A modified newton method for the solution of ill-conditioned systems of nonlinear equations with application to multiple shooting. *Numer. Math*, 22:289–315.

Echelmeyer, K. and Wang, Z. (1987). Direct observation of basal sliding and deformation of basal drift at sub-freezing temperatures. *Journal of Glaciology*, 33(113).

Engelhardt, H. and Kamb, B. (1998). Basal sliding of ice stream b, west antarctica. *Journal of Glaciology*, 44(147).

Ettema, J., van den Broeke, M. R., van Meijgaard, E., van de Berg, W. J., Bamber, J. L., Box, J. E., and Bales, R. C. (2009). Higher surface mass balance of the greenland ice sheet revealed by high-resolution climate modeling. *Geophys. Res. Lett.*, 36(12):L12501.

Fahnestock, M., Adbalati, W., Joughin, I., Brozena, J., and Gogineni, P. (2001). High geothermal heat flow, basal melt, and the orgin of rapid ice flow in central greenland. *Science*, 294:2338–2342.

Goldsby, D. L. and Kohlstedt, D. L. (2001). Superplastic deformation of ice: Experimental observations. *J. Geophys. Res.*, 106(B6):11017–11030.

Greve, R. (1997). Application of a polythermal three-dimensional ice sheet model to the greenland ice sheet: Response to steady-state and transient climate scenarios. *J. Climate*, 10(5):901–918.

Greve, R. (August 2005). Relation of measured basal temperatures and the spatial distribution of the geothermal heat flux for the greenland ice sheet. *Annals of Glaciology*, 42:424–432(9).

Hughes, J. R. (2000). *The Finite Element Method, Linear Static and Dynamic Finite Element Analysis.*

Huybrechts, P., Payne, T., and Group, T. E. I. (1996). The eismint benchmarks for testing ice–sheet models. *Ann. Glaciol.*, 23:1–12.

Joughin, I., Das, S. B., King, M. A., Smith, B. E., Howat, I. M., and Moon, T. (2008). Seasonal Speedup Along the Western Flank of the Greenland Ice Sheet. *Science*, 320(5877):781–783.

Joughin, I., Smith, B. E., Howat, I. M., Scambos, T., and Moon, T. (In press). Greenland flow variability from ice-sheet-wide velocity mapping. *Journal of Glaciology.*

Luthi, M., Funk, M., Iken, A., Gogineni, S. P., and Truffer, M. (2002). Mechanism of fast flow in jakobshavns isbrae, west greenland. part iii. measurements of ice deformation, temperature and cross-borehole conductivity in boreholes to the bedrock. *Journal of Glaciology*, 48(162):369–385.

MacAyeal, D. R. (1993). A tutorial on the use of control methods in ice-sheet modeling. *J. Glaciol.*, 39(131):91–98.

Oswald, G. K. A. and Gogineni, S. P. (January 2008). Recovery of subglacial water extent from greenland radar survey data. *Journal of Glaciology*, 54:94–106(13).

Paterson, W. and Budd, W. (1982). Flow parameters for ice sheet modeling. *Cold Regions Science and Technology*, 6(2):175–177.

Paterson, W. S. B. (1994). *The Physics of Glaciers*.

Pattyn, F. (2003). A new three-dimensional higher-order thermomechanical ice-sheet model: basic sensitivity, ice-stream development and ice flow across subglacial lakes. *Journal of Geophysical Research (Solid Earth)*, 108(B8):2382.

Price, S. F., Payne, A. J., Catania, G. A., and Neumann, T. A. (2008). Seasonal acceleration of inland ice via longitudinal coupling to marginal ice. *Journal of Glaciology*, 54(185):213–219.

Shapiro, N. M. and Ritzwoller, M. H. (2004). Inferring surface heat distributions guided by global seismic model: particular applications to antarctica. *Earth Planet. Sci. Lett.*, 223:69–84.

Strang, G. (2007). *Computation Science and Engineering*.

van de Wal, R. S. W., Boot, W., van den Broeke, M. R., Smeets, C. J. P. P., Reimer, C. H., Donker, J. J. A., and Oerlemans, J. (2008). Large and rapid melt-induced velocity changes in the ablation zone of the greenland ice sheet. *Science*, 321:111–113.

Weertman, J. (1968). Comparison between measured and theoretical temperature profiles of the camp century, greenland, borehole. Technical Report 246.

Zwally, H. J., Abdalati, W., Herring, T., Larson, K., Saba, J., and Steffen, K. (2002). Surface melt- induced acceleration of greenland ice-sheet flow. *Science*, 297:218–222.